P1.8

COMPARISON OF TORNADIC AND NON-TORNADIC SUPERCELLS USING THE NATIONAL WEATHER SERVICE'S GRAPHICAL FORECAST EDITOR

J. Brad McGavock*, Robert B. Darby, Steven F. Piltz, James M. Frederick

National Weather Service Forecast Office, Tulsa, Oklahoma

1. INTRODUCTION

The severe weather episodes of 12 March 2006 and 6 April 2006, which affected eastern Oklahoma and northwest Arkansas, exhibited similar synoptic and mesoscale environments, yet the magnitude of the observed severe weather was noticeably different. Specifically, the tornadic potential with both events was strongly worded in outlooks from both the Storm Prediction Center and the Weather Forecast Office (WFO) at Tulsa, Oklahoma, but only the 12 March 2006 event produced significant tornadoes. Only three weak short-lived tornadoes occurred within the WFO Tulsa County Forecast and Warning Area (CFWA) on 6 April 2006.

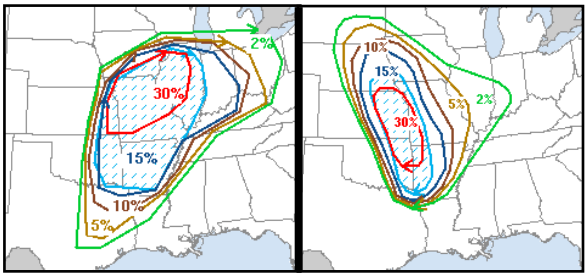

Figure 1: 12 March 2006 (left) and 6 April 2006 (right) 2000 UTC SPC Day 1 Tornado Outlook

The near-storm environments of the two most organized supercells from these events, one tornadic and the other non-tornadic (**Appendix A**), will be compared and contrasted within the National Weather Service's Graphical Forecast Editor (GFE). Computer scripts executed in GFE, referred to as SmartTools, allow for high resolution calculation and display of severe weather parameters. Additionally, recent additions to the toolset allow hodographs to be generated using observed storm motions. The hodographs are displayed along with vertical plots of the associated environmental and storm-relative wind profiles. The functionality of this SmartTool will be featured in the analysis.

2. UTILIZING GFE

The National Weather Service's (NWS) Graphical Forecast Editor (GFE; Forecast Systems Laboratory 2001) is being utilized at WFO Tulsa not only to generate forecast products, but also as an interactive mesoscale objective analysis tool. The latter utilizes computer scripts that meld observed and objectively analyzed surface data with numerical model data. Results allow environmental parameters classically associated with severe local storm forecasting, such as instability, helicity, and shear, to be generated (McGavock, et. al. 2004). These data are produced on a 2.5 km x 2.5 km grid, where the integrity of the observed values is maintained. Variations on the classical parameters can also be calculated and displayed, such as storm-relative helicity (SRH) computed to the lifting condensation level (LCL) rather than to an arbitrary height. A forecaster can produce either an analysis of the current hour (as is done by other schemes that mix observed surface data with model data from higher levels) or produce forecast fields after adjusting for biases in model surface data. The SRH calculations utilize a user-defined storm motion grid instead of an assumed motion, which is often unrepresentative. The most recent convective SmartTool developed at WFO Tulsa also incorporates this user-defined storm motion to produce storm-specific hodographs coupled with environmental and storm-relative wind profiles. This tool has the ability to be executed over any number of grid points within the WFO Tulsa GFE domain, allowing hodograph representations from regional averages to near-storm environments.

3. SYNOPTIC

The synoptic upper air patterns of both 12 March 2006 and 6 April 2006 exhibited pronounced troughing progressing into the central United States, with 250 hPa jet streaks overspreading the Southern Plains (not shown). The 500 hPa patterns on both events (Figure 2) produced winds in excess of 70 kts across eastern Oklahoma and northwest Arkansas by 0000 UTC, with an open, positively tilted trough on 12 March 2006 and a closed low within a negatively tilted trough on 6 April 2006.

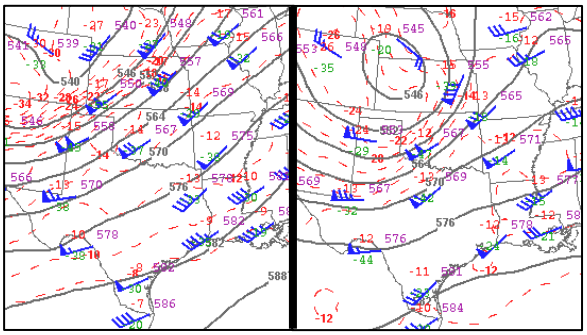

Figure 2: 0000 UTC 13 March 2006 (left) and 7 April 2006 (right) 500 hPa analysis (obtained via SPC)

* Corresponding author address: J. Brad McGavock, National Weather Service, Tulsa, OK 74128-3050; E-mail: brad.mcgavock@noaa.gov

The 700 hPa pattern (Figure 3) reflected the strength of the wind fields, with both events exhibiting speeds in excess of 40 kts at 0000 UTC across much of the Southern Plains, with speeds of 50 kts or greater across portions of eastern Oklahoma and northwest Arkansas based on Haskell, Oklahoma Wind Profiler data. Greater cyclonic curvature within the 6 April 2006 overall pattern was evident at 700 hPa, with a longer fetch of southwesterly flow noted on 12 March 2006. This difference was most notable across eastern Kansas and west Texas, with lesser directional difference noted across eastern Oklahoma and northwest Arkansas.

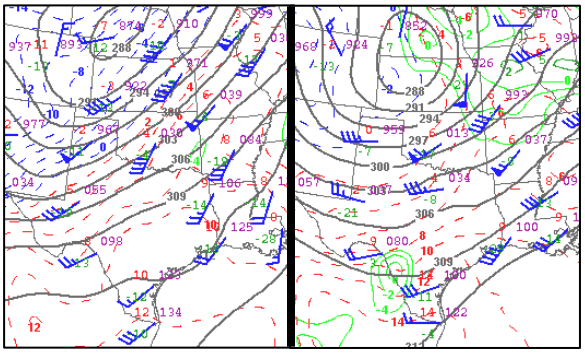

Figure 3: 0000 UTC 13 March 2006 (left) and 7 April 2006 (right) 700 hPa analysis (obtained via SPC)

The 850 hPa pattern (Figure 4) was largely similar in both events, as observed 0000 UTC data revealed southerly winds of 30 to 40 kts in proximity to eastern Oklahoma and northwest Arkansas, along with a moisture axis centered from east Texas through eastern Oklahoma. The most notable difference was the magnitude of the 850 hPa dewpoints; 12ºC to 14ºC dewpoints were analyzed across eastern Oklahoma on 0000 UTC 13 March 2006, whereas dewpoints of 10ºC to 12ºC were analyzed on 0000 UTC 7 April 2006 across the same region.

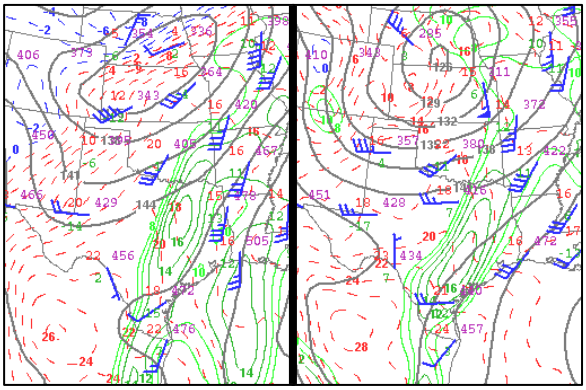

Figure 4: 0000 UTC 13 March 2006 (left) and 7 April 2006 (right) 850 hPa analysis (obtained via SPC)

The surface pattern between both events (Figure 5) featured distinct warm and cold fronts, with a well-defined dryline advancing into eastern Oklahoma by the late afternoon hours on both dates. The strength and track of the surface low differed between the two events, with the 12 March 2006 surface low tracking across central Kansas, while the surface low was stronger and tracked from northern Kansas into southern Nebraska on 6 April 2006.

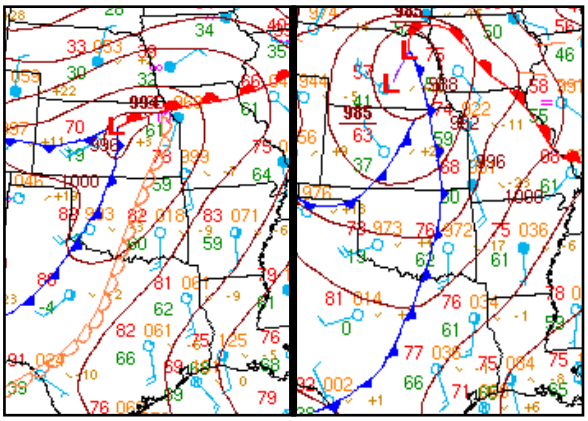

Figure 5: 0000 UTC 13 March 2006 (left) and 7 April 2006 (right) Surface analysis (obtained via SPC)

4. MESOSCALE

A dryline was the focus for thunderstorm initiation across eastern Oklahoma for both the 12 March 2006 and 6 April 2006 events, though initiation times differed by several hours. The 12 March 2006 event displayed stronger inhibition throughout the tornadic portion of the event, with the more widespread thunderstorm coverage delayed until the passage of a cold front. The 6 April 2006 event featured more widespread erosion in inhibition along the dryline by early afternoon, with thunderstorm coverage increasing soon after initiation.

An axis of potential instability immediately east of the dryline was apparent in both events, with lifted index values of -3 to -5ºC (shown by dark blue in Figure 6) common along a narrow corridor. The eastward extent of the stronger potential instability was also limited during both events, with lifted index values of 0º to -2ºC maintained across northwest Arkansas, corresponding to lesser lower-level moisture values. The potential instability axis did attempt to shift eastward with time as the dryline progressed; however, both events featured mature supercells advancing through and approaching the eastern extent of the potential instability axis during the strongest portions of their lifecycle.

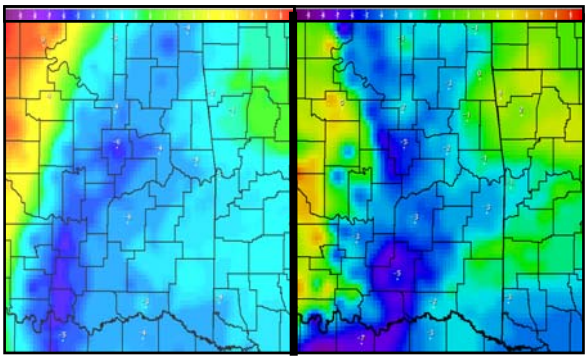

Figure 6: 0000 UTC 13 March 2006 (left) and 7 April 2006 (right) Lifted Index (blue colors are most unstable)

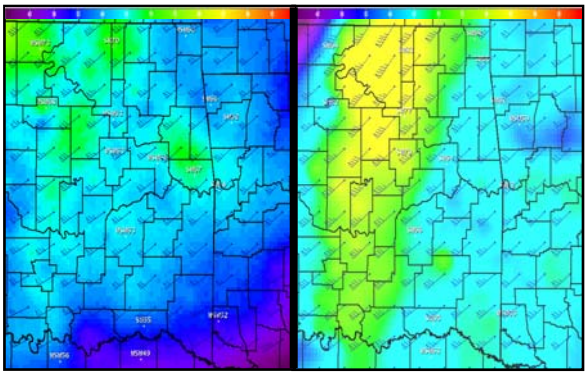

Figure 7: 0000 UTC 13 March 2006 (left) 7 April 2006 (right) 0-6km Shear (warmer colors indicate higher values)

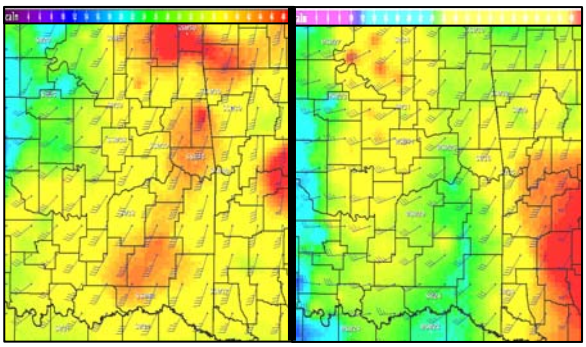

Figure 8: 0300 UTC 13 March 2006 (left) and 0000 UTC 7 April 2006 (right) 0-1km Shear (warmer colors indicate higher values)

5. NEAR-STORM ENVIRONMENTS

GFE allows the analysis of near-storm environments, specifically the ability to incorporate observed storm motions into storm-relative wind and helicity calculations. WFO Tulsa has developed a SmartTool that generates storm-specific hodographs and relative wind information as seen in Figures 9 and 10. The left axis on the display is an environmental wind profile utilizing observed surface data and numerical model data. The right axis displays the storm-relative wind profile, which along with the hodograph, utilizes a user-defined storm motion. Use of observed storm motions better capture the highly variable SRH environment (Markowski, et al. 1998) and produce more representative storm-relative wind profiles (Storm Prediction Center MesoAnalysis Overview). The SmartTool can operate over any range of selected points within the GFE domain.

The convective mode with both events was predominately supercellular given 0-6 km shear values in excess of 50 kts (Thompson et. al. 2003). Cellular interaction was limited as the deep layer shear vectors attained a sufficient perpendicular component to the surface dryline (Figure 7). Low-level wind fields with both events also produced shear values supportive of tornadic potential (Thompson et. al. 2003), and both events displayed upward trends in 0-1km shear values downstream in the hours ahead of the strongest supercells. Figure 8 shows the 0-1 km shear fields for both dates valid at the hour nearest the most intense radar imagery of the ongoing supercells.

The near-storm environments from the two most well organized supercells from 12 March 2006 and 6 April 2006 were analyzed through GFE. Each environment was characterized by SRH values supportive of tornadic potential (Thompson et. al. 2003).

The 13 March 2006 0300 UTC hodograph (Figure 9) was produced utilizing observed surface data and zero hour Rapid Update Cycle (RUC) data to reflect the environment across southern Delaware County near the time the first of two F3 tornadoes (Fujita 1972). The large amount of curvature noted within the lowest portions of the hodograph represents an increase in wind speeds to near 60 kts within the 1-2 km above ground level (AGL) layer. The use of RUC upper air data was supported by observations from the KSRX and KINX Weather Surveillance Radar - 1988 Doppler (WSR-88D) Velocity Azumith Displays. This produced 0-1 km SRH values greater than 550 $m^2 s^{-2}$. Additionally, the storm-relative inflow (shown on the right axis) within the 0-1 km AGL layer reached 55 kts, along with pronounced veering with height.

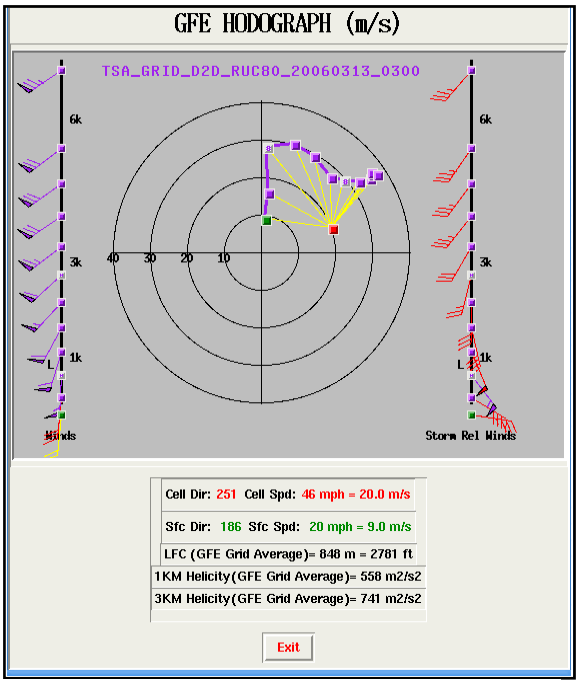

Figure 9: 0300 UTC 13 March 2006 hodograph ($m\ s^{-1}$), environmental wind (kts), and storm-relative wind (kts) display produced via GFE

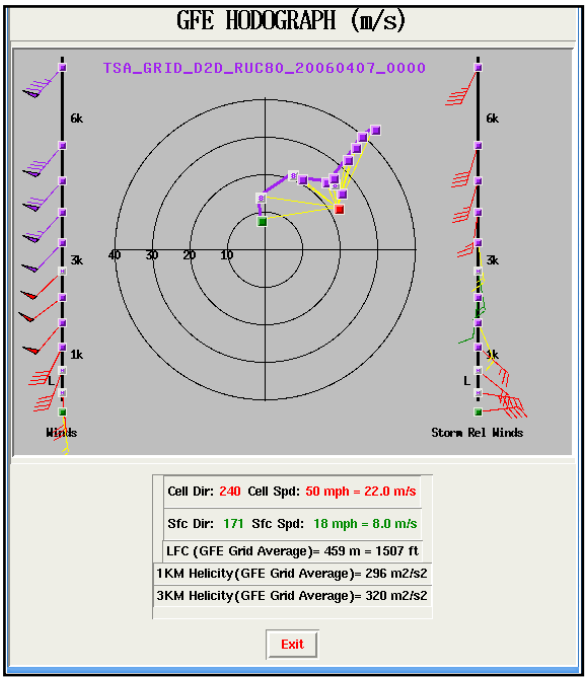

Figure 10: 0000 UTC 7 April 2006 hodograph ($m\ s^{-1}$), environmental wind (kts), and storm-relative wind (kts) display produced via GFE

The 7 April 2006 0000 UTC hodograph (Figure 10) was produced to reflect the environment across southern Mayes County using RUC upper-air and observed surface data. The environmental wind profile (shown on the left axis) was similar to the 12 March 2006 event with the notable exception being the speeds within the 0-1 km AGL layer. The hodograph exhibits low-level curvature that, when combined with the observed storm motion, yields 0-1km SRH values near 300 $m^2\ s^{-2}$. The storm-relative wind profile (shown on the right axis) exhibits pronounced veering within the 0-1 km AGL layer similar to the 12 March 2006 event; however, the magnitudes within this layer are approximately 10 to 15 kts less. The comparable weakness in storm-relative winds also extends into the 1-3 km AGL layer, with magnitudes falling below 10 kt near 2 km AGL. Additionally, the degree of veering within the 1-3 km AGL layer becomes noticeably less.

6. RADAR EVOLUTION

6.1 Non-tornadic Supercell

Isolated supercells developed by 2200 UTC on 6 April 2006 across eastern Oklahoma, with one such storm attaining classic supercellular structure as it passed within 18 km of the KINX WSR-88D radar. This close pass to the radar provided well defined reflectivity and velocity data and allowed for the detection of sub-cloud base rotation. This storm initially developed over southern Tulsa County around 2300 UTC, before moving into far southwest Mayes County by 2350 UTC, where it developed a pronounced hook echo (Figure 11). A deep mesocyclone was noted at this time with a depth to 3.1 km (10 kft) AGL. The mesocyclone diameter was approximately 9 km across, with 15 $m\ s^{-1}$ (30 kt) maximum rotational velocity. A three-dimensional analysis of the supercell at this time, using GRLevel2 Analyst Edition (AE) software (Gibson Ridge Software), showed the updraft to be tilted with height, along with an ill-defined weak echo region aloft (Figure 12). The 0003 UTC 7 April 2006 data show the rear-flank downdraft (RFD) had surged east ahead of the mesocyclone, followed by the storm becoming increasingly unorganized. The disorganization in structure led to a continued weakening trend across Delaware County, which also corresponded to the storm moving into an environment of lesser surface-based instability.

6.2 Tornadic Supercell

Supercells on 12 March 2006 initiated near 0100 UTC across eastern Oklahoma. The supercell of focus developed over southern Tulsa County near 0200 UTC, with gradual organization and intensification between 0200 UTC and 0300 UTC. The supercell exhibited several anticyclonic mesocyclone splits, which rapidly weakened, while the cyclonic mesocyclone persisted and strengthened with increasing low-level reflectivity and velocity structure.

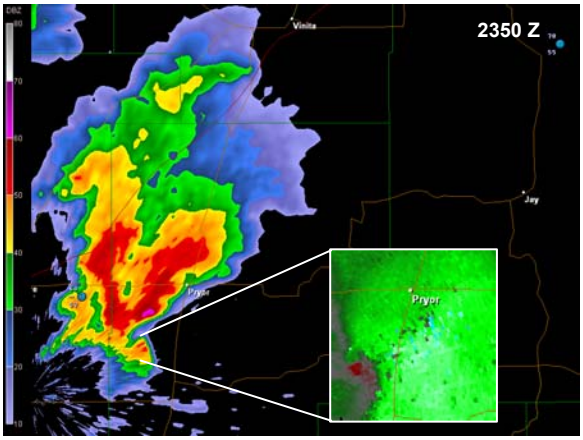

Figure 11: 2350 UTC 6 April 2006 KINX WSR-88D 0.5º reflectivity and storm relative velocity insert. Displayed in GRLevel2 AE.

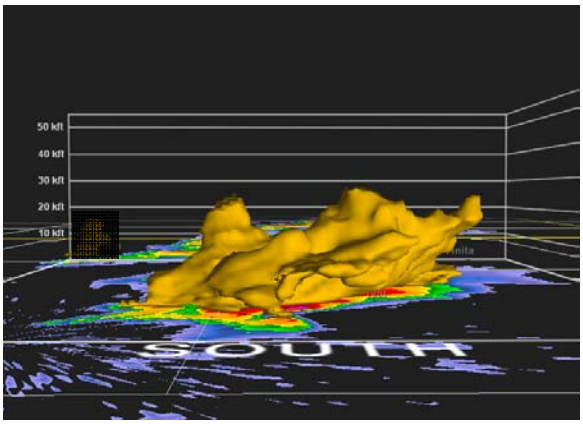

Figure 12: 2350 UTC 6 April 2006 KINX WSR-88D 45 dBz isosurface. Displayed in GRLevel2 AE looking north.

The supercell moved into northern Cherokee County by 0324 UTC and developed a mesocyclone depth to 7.6 km (25 kft) AGL. At this time there was a rapid increase in low level rotation with maximum rotational velocities of 31 m s^{-1} (60 kts) across 4 km. This period of cyclic mesocyclone organization prior to tornadic development was viewed as typical of mature supercells. The initial tornado developed in northern Cherokee County and tracked northeast into southern Delaware County, causing F3 damage. Figure 13 shows the strong velocity couplet within the hook echo region of the supercell near its peak radar presentation and during the time of the initial tornado. This long-lived tornadic supercell continued northeast into northwest Arkansas and produced three additional tornadoes of F3, F2, and F1 magnitude, respectively (**Appendix A**).

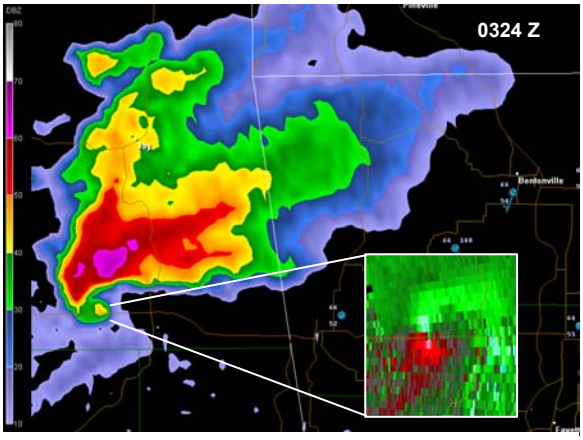

Figure 13: 0324 UTC 13 March 2006 KINX WSR-88D 0.5º reflectivity and storm relative velocity insert. Displayed in GRLevel2 AE.

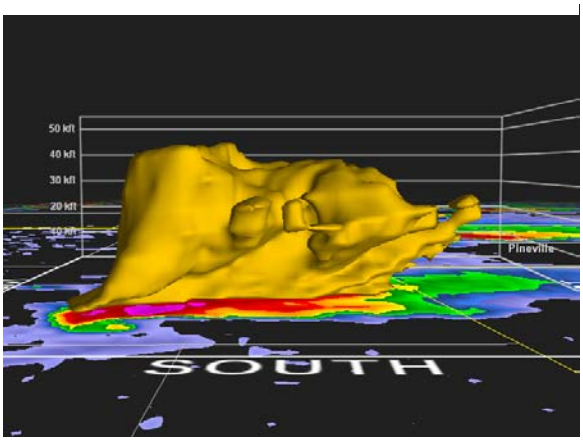

Figure 14: 0324 UTC 13 March 2006 KINX WSR-88D 45 dBz isosurface. Displayed in GRLevel2 AE looking north.

7. Supercell Comparison

The updraft in the 12 March 2006 supercell is more upright than the 6 April 2006 supercell as seen in the three-dimensional imagery (Figure 12 and 14), despite similar deep layer shear magnitudes. The variance in supercell organization and resultant severe weather production between the 12 March 2006 and 6 April 2006 was considered difficult to anticipate given the synoptic and mesoscale similarities. The GFE hodograph and storm-relative wind SmartTool was not available for real-time diagnosis during these events, yet when utilized for the case review, revealed significant environmental differences. One possible explanation is that the weakness in storm-relative winds within the 1-2 km layer on 6 April 2006, as shown by green and yellow wind barbs in Figure 10, did not allow initial mesocyclone attempts to attain sufficient strength to significantly enhance the updraft. This lack of updraft efficiency, likely due to precipitation loading, was

further complicated by marginal surface-based instability (Brooks et al.). This lack of updraft organization occurred within an otherwise favorable storm-relative helicity environment, as the degree of cyclonic curvature noted within Figure 10 would suggest.

The 12 March 2006 storm-relative wind profile supported an environment favorable for initial mesocyclones to strengthen and, when juxtaposed with the surface potential instability axis, yielded an updraft with increasing strength. The hodograph prior to tornado production highlighted the degree of low-level curvature, which was significantly more pronounced than during the 6 April 2006 event. The strength of the updraft associated with the tornadic supercell was evident not only in its cyclic tornado production, but also with its ability to maintain strength well east of the surface potential instability axis.

8. SUMMARY

The comparison of severe weather events on 12 March 2006 and 6 April 2006, along with individual supercells within these environments, illustrate the range of observed severe weather within comparable synoptic and mesoscale patterns. The ability to interact with observed data, such as specific storm motions, within GFE has proven useful at WFO Tulsa toward diagnosing the subtleties each severe weather event possesses. The most recent addition to WFO Tulsa's GFE convective SmartTools adds to the ability of diagnosing the near-storm environment, specifically analyzing storm-relative winds and their relationship to the hodograph. The variability associated with correctly diagnosing the storm-relative environment is, in part, captured by GFE's functionality to effectively and efficiently incorporate user-defined datasets. The two events discussed highlight the importance of being able to interact with these data, impacting both severe weather outlooks and warning decisions.

9. ACKNOWLEDGEMENTS

The authors would like to thank Frank Mitchell of KTUL Channel 8 in Tulsa, Oklahoma for his efforts toward attaining archived spotter video from 6 April 2006.

10. REFERENCES

Brooks, H. E., 1993. The Role of Midtropospheric Winds in the Evolution and Maintenance of Low-Level Mesocyclones. *Monthly Weather Review*. **122:** 126-136.

Fujita, T. T., 1972: A proposed characterization of hurricanes and tornadoes by area and intensity. SMRP Paper 91, 42 pp., Univ. of Chicago.

Hansen, T.L., M. Mathewson, and M. Romberg. 2000. Forecast Methodology using the GFESuite. Preprints, *17th International Conference on Interactive Information and Processing Systems for Meteorology, Oceanography, and Hydrology*. American Meteorological Society.

Gibson Ridge Software. 2006 October 30. GRLevelX homepage. <http://www.grlevelx.com>. Accessed 2006 October 30.

McGavock, J.B., S. Piltz, and J. Frederick. 2004. Interactive Mesoscale Objective Analysis in the National Weather Service's Graphical Forecast Editor, Preprints, *22nd Conference on Severe Local Storms*. American Meteorological Society.

Markowski, P.M., J. Straka, E.N. Rasmussen, and D.O. Blanchard. 1998. Variability of Storm-Relative Helicity during VORTEX. *Monthly Weather Review.* 126: 2959-2971.

Thompson, R.L., R. Edwards, J.A. Hart, K.L. Elmore, and P.M. Markowski. 2003. Close Proximity Soundings within Supercell Environments Obtained from the Rapid Update Cycle. *Weather and Forecasting.* 18: 1243-1261.

Storm Prediction Center MesoAnalysis Overview. 2006 October 30. SPC MesoAnalysis Homepage. <http://www.spc.noaa.gov/exper/mesoanalysis/>. Accessed 2006 October 30.

Appendix A: WFO Tulsa CFWA with supercell tracks plotted from 06 April 2006 and 12 March 2006, including F1 or greater tornado tracks. KINX and KSRX WSR-88D locations also plotted.